Environmental Science & Technology

ARTICLE

pubs.acs.org/est

Effects of Income and Urban Form on Urban NO_2: Global Evidence from Satellites

Matthew J. Bechle,[†] Dylan B. Millet,[†,‡] and Julian D. Marshall[*,†]

[†]Department of Civil Engineering, University of Minnesota, Minneapolis, Minnesota 55455, United States

[‡]Department of Soil, Water, and Climate, University of Minnesota, Minneapolis, Minnesota 55455, United States

S *Supporting Information*

ABSTRACT: Urban air pollution is among the top 15 causes of death and disease worldwide, and a problem of growing importance with a majority of the global population living in cities. A important question for sustainable development is to what extent urban design can improve or degrade the environment and public health. We investigate relationships between satellite-derived estimates of nitrogen dioxide concentration (NO_2, a key component of urban air pollution) and urban form for 83 cities globally. We find a parsimonious yet powerful relationship (model $R^2 = 0.63$), using as predictors population, income, urban contiguity, and meteorology. Cities with highly contiguous built-up areas have, on average, lower urban NO_2 concentrations (a one standard deviation increase in contiguity is associated with a 24% decrease in average NO_2 concentration). More-populous cities tend to have worse air quality, but the increase in NO_2 associated with a population increase of 10% may be offset by a moderate increase (4%) in urban contiguity. Urban circularity ("compactness") is not a statistically significant predictor of NO_2 concentration. Although many factors contribute to urban air pollution, our findings suggest that antileapfrogging policies may improve air quality. We find that urban NO_2 levels vary nonlinearly with income (Gross Domestic Product), following an "environmental Kuznets curve"; we estimate that if high-income countries followed urban pollution-per-income trends observed for low-income countries, NO_2 concentrations in high-income cities would be ~10× larger than observed levels.

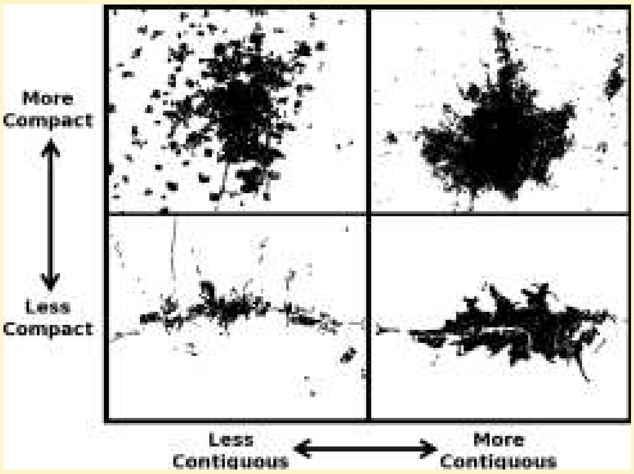

INTRODUCTION

Urban air pollution is responsible for an estimated 1 million deaths annually, or approximately 17% of environmentally related deaths in low- and middle-income countries and 81% in high-income countries.[1] In 2008, for the first time in history, urban dwellers outnumbered rural dwellers; in coming decades, urban populations are expected to double while rural populations remain constant or decline.[2] In recent decades, urban air quality has improved for many pollutants in developed countries, but declined in most developing countries for reasons that include rapid urban growth, strained transportation infrastructure, increased congestion and automobile ownership, and lack of effective emission control policies.[3,4] Motor vehicles are a major contributor to urban air pollution. For instance, motor vehicles account for approximately half (53%) the emissions of nitrogen oxides ($NO_x \equiv NO + NO_2$) in U.S. urban areas (based on the U. S. EPA National Emissions Inventory [http://www.epa.gov/ttn/chief/emch/index.html#2005] and urban area boundary files from the 2000 U.S. Census [http://www.census.gov/geo/www/ua/ua_bdfile.html]). Strategies for reducing vehicular emissions include changing vehicles, fuels, or vehicle activity level (e.g., annual average travel-distance per vehicle). Vehicle activity level is correlated with the size, shape, and layout of a neighborhood or city—i.e., its urban form.[5−10] For example, evidence suggests that daily vehicle travel distances are less for residents of denser urban areas than for residents of less dense areas; in high-density areas, on average, origins and destinations are closer together, mass-transit is more available, and disincentives to driving, such as congestion and parking fees, are greater.[11] This observation implies that increasing population density may decrease vehicle-kilometers traveled, reduce motor vehicle emissions, and consequently, improve air quality.[12−14] More densely populated and geometrically compact and contiguous cities might therefore be expected to have reduced vehicle emissions and cleaner air.

Received: November 16, 2010
Revised: February 18, 2011
Accepted: March 8, 2011
Published: May 04, 2011

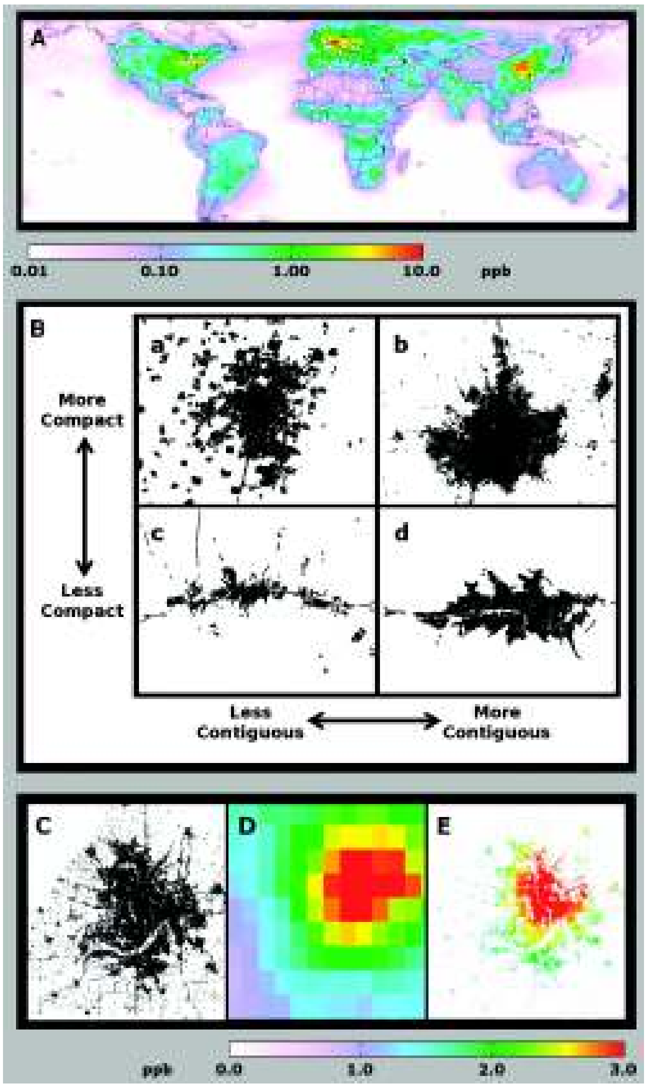

Figure 1. Global and urban-scale NO_2 concentrations in surface air. (A) Three-year average NO_2 concentrations for the world at $0.1° \times 0.1°$ resolution derived from satellite measurements. Circles indicate the 83 global cities included in this study. (B) Contiguity (urban patchiness) and compactness (circularity of the main built-up area) illustrated by (a) Changzhi, China (0.33, 0.45 for contiguity and compactness respectively); (b) Ibadan, Nigeria (0.94, 0.47); (c) Malatya, Turkey (0.36, 0.22); (d) Jequié, Brazil (0.98, 0.25). For one of the urban areas (Minneapolis-St. Paul, Minnesota, USA), (C) built-up areas (resolution: 0.1×0.1 km^2), (D) three-year average surface NO_2 concentration (resolution: $0.1° \times 0.1°$, or about 8×11 km^2), and (E) three-year average NO_2 concentrations, formed by combining and interpolating (C) and (D) (resolution: 0.1×0.1 km^2). Non built-up areas are not considered in the analyses.

However, increasing population density with the aim of reducing vehicle emissions creates a counterintuitive potential hazard: even if emissions decline, air pollution concentrations and population exposure may worsen since people and their vehicles' emissions are closer together. Shifts in urban form could thus reduce vehicle emissions yet increase primary pollutant concentrations.[15,16] The net effect of high- versus low-density development on air quality is thus a balance of competing changes in emissions and atmospheric dilution.[15]

In addition to the emission–dilution trade-off, the wealth of a city may influence its air quality. The environmental Kuznets curve (EKC) suggests that rising income increases pollution when per capita gross domestic product (GDP) is low, but decreases pollution when per capita GDP is high.[17−19] This relationship is often attributed to the transition of a society from agrarian to industrialized and finally to a service economy.[20] A related explanation involves the competing effects of scale and technology:[17] as a developing economy experiences rapid growth, it increases output and consequently increases emissions; economic growth leads to technological progress, which allows cleaner new technologies to replace dirtier obsolete technologies, thus improving environmental quality. This phenomenon occurs over long periods of time for a single country, but it is also observed in multicountry cross-sectional analyses.[17,18] The EKC hypothesis holds in many cases (especially for urban air pollution) but it is not universal.[18,21,22]

Here we employ satellite measurements of nitrogen dioxide (NO_2, a key component of urban air pollution) from the Ozone Monitoring Instrument (OMI[23]) and a global data set of 83 urban areas (Figure 1A) to explore the relationship between urban form and air pollution concentrations. We also examine relationships between income and satellite-estimated air pollution concentrations. Most prior investigations exploring the relationship between urban form and air quality have been modeling studies, relying on projected growth and land use scenarios to model air quality outcomes for specific cities.[24−28] The few prior empirical studies generally focus on a single country and are limited to developed countries where high quality atmospheric and land use data are available.[14,16,29] We present the first study using satellite measurements to explore the urban form–air pollution relationship for a stratified global sample of cities.

Although NO_2 is mainly produced in the atmosphere from photochemical oxidation of directly emitted nitric oxide (NO), the time scale for that transformation is short (minutes), so that NO_2 concentrations are essentially a marker for combustion-related emissions. Major sources of combustion-related emissions in urban areas are transportation, power generation, and industrial processes. Biomass burning can also contribute significantly to combustion emissions in nonurban regions (e.g., wildfires and human-initiated burning for land clearing) and developing countries (e.g., cooking and heating). NO_2 is linked to numerous adverse health effects[30−33] including lung cancer,[34] cardiopulmonary mortality,[35] and type 2 diabetes.[36] NO_2 is environmentally important as a marker for combustion emissions, as a precursor to the formation of ground-level ozone and particulate matter, because it has direct health effects, and as a cause of acid rain. NO_2 is a criteria pollutant regulated in the U.S. Clean Air Act. Here we show quantitatively that urban design can influence NO_2 concentrations, and demonstrate that urban NO_2 levels around the world track the wealth of the city in a nonlinear way and according to an EKC.

METHODS

While high quality, in situ measurements of urban air pollution are conducted regularly and are publicly available for many developed countries, such data are lacking for most developing countries. In contrast, satellite measurements offer near-global coverage using a uniform methodology.[37−39] Data quality is consistent across cities, regions, and countries, and devoid of the political biases sometimes observed for in situ measurements.[40−42] OMI provides daily measurements of NO_2 atmospheric column abundance. We derive daily surface concentrations using NO_2 surface-to-column ratios from a global chemical transport model

Table 1. Summary Statistics among the 83 Cities

	mean	SD[a]	GM[b]	GSD[c]	interquartile range
arithmetic mean NO_2 (ppb)	2.0	2.6	1.0	3.4	0.41−3.0
population (million)	2.7	3.8	1.3	3.0	0.56−2.8
income (US$)	$9,600	$10,000	$5,400	3.3	$2,300−$18,000
contiguity index	0.71	0.20	0.67	1.4	0.59−0.89
compactness index	0.35	0.10	0.33	1.4	0.27−0.43
harmonic mean dilution rate ($m^2\ s^{-1}$)	2,600	2,600	1,500	3.1	520−4,300

[a] Standard deviation. [b] Geometric mean. [c] Geometric standard deviation, unitless.

Table 2. Linear Regression Model for Logarithm of Mean Urban NO_2

	coefficient	std. error	$P < \|t\|$	Δ (1 − SD ↑)[a]	Δ(1 − SD ↓)[a]
constant	−2.4	0.47	<0.001	--	--
income (US$)	6.5×10^{-5}	1.7×10^{-5}	<0.001	−22%	−22%
(income)^2	-1.1×10^{-9}	5.5×10^{-10}	0.05		
log (population)	0.41	0.074	<0.001	62%	−38%
contiguity	−0.58	0.19	0.004	−24%	31%
compactness	0.19	0.37	0.62	4.6%	−4.4%
harmonic mean dilution rate ($m^2\ s^{-1}$)	-4.6×10^{-5}	1.5×10^{-5}	0.003	−24%	31%

[a] Change in surface NO_2 concentration for a one standard deviation increase/decrease from mean value while all other independent variables are held at mean values. For income: percent change for a one standard deviation increase/decrease from the peak NO_2 value (income = $29,600) while all other independent variables are held at mean values.

[GEOS-Chem,[43] see Supporting Information (SI) for details] for a 3-h window (12:00−15:00 local time) corresponding to satellite overpass time. Figure 1A shows global NO_2 surface concentrations derived in this way from the OMI measurements, averaged over three years (2005−2007) and for visual display gridded to 0.1° × 0.1° (∼11 × 11 km^2 at the equator) resolution. OMI-derived NO_2 surface estimates are typically lower than 24-h average in situ measurements; reasons include spatial averaging from the satellite pixel and GEOS-Chem model, chemical interferences for certain in situ NO_2 measurements,[40] and the diurnal cycle of NO_2 in surface air. Lamsal et al.[40] demonstrated that the approach employed here to derive surface NO_2 concentrations from the satellite data gives values that are well-correlated with in situ observations.

To understand and quantify the impact of urban form and income on air pollution, we use data from the World Bank's Urban Growth Management Initiative to define urban extent and characteristics for a stratified global sample of 83 cities (Figure 1A). All cities with available data were used for this analysis. The data set is based on Landsat satellite imagery and land use classification, and provides estimates of population, built-up area, per capita GDP (income), contiguity, and compactness[44] for metropolitan areas. Urban extent is defined by built-up area determined from land use classification of Landsat images, rather than administrative borders. Using this definition, built-up area and urban extent excludes some areas (e.g., parks and other green spaces) that might often be considered part of the city. As employed in this paper, the terms "compactness" and "contiguity" refer to the geometric shape of a city and have a more precise meaning than in common usage. Contiguity is a measure of urban patchiness (degree of "leapfrog" development), calculated as the ratio of the main contiguous built-up area to the total built-up area of the city. Compactness is a measure of the circularity of the main built-up area of a city, calculated as the ratio of built-up area to total buildable area (areas without bodies of water or extreme slopes) within a circle surrounding the main built-up area of the city. The urban form characteristics we use from this data set represent a subset of the dimensions typically used to classify urban form; other urban form characteristics (e.g., land use mix, road network density, and centrality with respect to population and/or employment) are not included in this analysis because they are not available at a global scale. For a recent discussion of satellite-based estimates of land use, see Potere et al.[45] Figure 1B illustrates contiguity and compactness using four cities in the study. We employ a meteorology metric (harmonic mean of the dilution rate at overpass time; dilution rate is the product of wind-speed and mixing height) to account for the influence of atmospheric dilution on pollution concentrations in each city.

Three-year annual-average surface mixing ratios for NO_2 derived from the OMI satellite measurements were interpolated to a 0.1 × 0.1 km^2 grid of built-up area for each city. We computed four measures (arithmetic mean, median, 90th percentile, and concentration-weighted mean) of NO_2 in each urban area; in each case, concentrations were log-normally distributed among cities. Arithmetic mean NO_2 mixing ratios vary from 0.07 to 16 ppb for the 83 cities, with an overall mean (standard deviation) of 2.0 (2.6) ppb and geometric mean (geometric standard deviation) of 1.0 ppb (3.4). Figure 1C−E illustrates built-up area and NO_2 concentrations for one of the 83 cities. Summary statistics for variables in the core model are provided in Table 1; summary statistics for all variables are provided in Table S1.

RESULTS AND DISCUSSION

We constructed a linear regression model (Table 2) for the logarithm of arithmetic mean NO_2 concentration in each city to determine its dependence on the urban characteristics. The resulting model captures more than 60% of the variability in the dependent variable (R^2 = 0.63, see Figure S1). Given the small number of parameters in the model and the variability in air

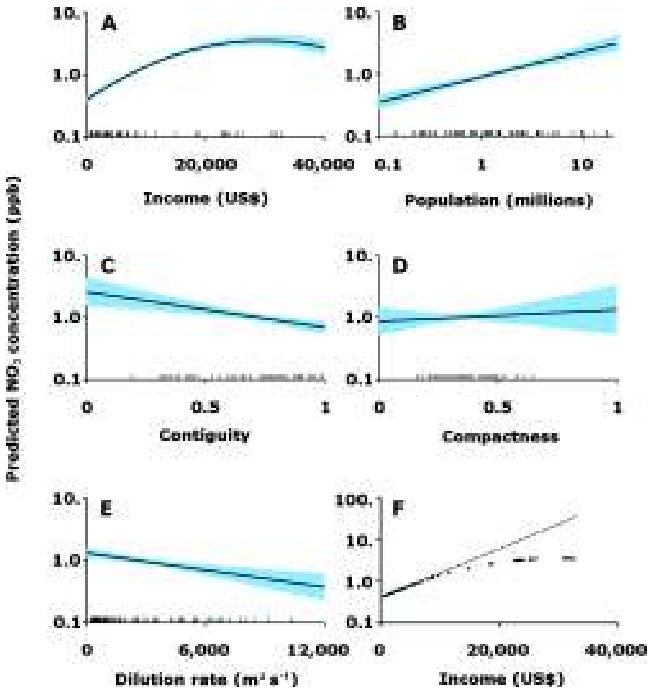

Figure 2. Unique effect of independent variables for the linear regression model (log−linear plots). (A−E) NO_2 concentration response for each independent variable while other independent variables are held at mean values. Shaded blue regions indicate 95% confidence intervals. Hash marks along the x-axes indicate independent variable value for each of the 83 cities. (F) Linear projection of predicted NO_2 concentration based on the lowest 50th percentiles of cities by income. Actual NO_2 concentrations in cities toward the upper end of the income distribution are an order of magnitude lower than the linear projection we show here.

pollution levels, the model offers a simple yet powerful description of underlying trends in the data. Figure 2 presents model-derived relationships between the dependent and independent variables. Employing mean values for all parameters (geometric mean for population) yields a concentration of 1.0 ppb.

We find that population has the single strongest effect on urban NO_2 levels and their differences among cities. Using mean values for the independent variables, a one geometric standard deviation population increase, 3.1 million people, would raise NO_2 concentrations by 62% (Figure 2B). The next largest effect in the model (aside from meteorology) is urban contiguity, with leapfrog development associated with higher NO_2 concentrations (a one standard deviation contiguity decrease yields a 31% increase in surface NO_2; $p = 0.004$. The results suggest that the average increase in NO_2 concentration associated with a population increase of 10% could be offset by a more contiguous urban landscape (specifically, by a 0.03-unit [on average 4%], increase in contiguity). Stated differently, the results suggest that a 3× increase (i.e., a one geometric standard deviation [GSD] increase) in population would yield a 62% (0.4-GSD) increase in NO_2 concentration, an amount that our model suggests could be offset by a 1.8-SD (0.34-unit; on average, 48%) increase in contiguity.

In contrast, the compactness index has no statistically significant impact on urban NO_2 levels. This finding may reflect a dilution/emissions trade-off, i.e., the degree to which emission reductions caused by the city's geometric compactness are masked by the increased proximity.[15] In addition, the compactness index is based on the circularity of the city; circular cities may or may not be

Table 3. Transition Points for Air Pollution Environmental Kuznets Curve Studies[a]

	sulfur dioxide	suspended particulate matter	carbon monoxide	nitrogen oxides
		emission-based studies		
ref 47	9,100	9,700	13,100	19,500
ref 48	14,200	12,700	25,300	28,900
		concentration-based studies		
ref 17	5,400			
ref 49	5,400			
ref 50	6,600			
ref 51	4,900	4,900		
this work				$29,600

[a] Adapted from Barbier.[46] Values are in year-1995 US dollars using GDP implicit price deflator method.

the most energy-efficient, or pollution-efficient, urban form. Contiguity and compactness are not well correlated (in our data set, $R^2 = 0.03$). Employing instead a multiple linear regression that excludes contiguity degrades the overall model performance (to $R^2 = 0.59$) and the significance of the compactness index (to $p = 0.99$), further indicating that compactness is not a proxy for contiguity. Likewise, population density was not identified in the model as statistically significant ($p = 0.12$), nor as providing an improvement to model performance (R^2).

We find a strong relation between income and air pollution across the 83 global cities (Figure 2A), consistent with the inverse "U" shape of the EKC. The peak occurs at approximately US $30,000 per capita GDP. Starting at this peak and employing mean values for all other independent variables, a 1-SD increase or decrease in per capita GDP yields a 22% reduction in NO_2 concentrations. This finding suggests a nonlinear relationship between pollution concentrations and urban economic development. The NO_2−income curve in Figure 2A can also be interpreted to define, in a globally integrated sense, a transition point in advanced urban development when cities start to become less polluting with increased economic growth. The ~$30,000 peak, derived here based on NO_2 concentrations, is broadly consistent with reported transition points derived using per capita NO_x emission estimates, but higher than for other air pollutants previously studied (see Table 3).

Figure 2F shows a linear projection based on the model relationship between income and surface NO_2 concentrations for the lowest 50th percentiles of cities by income. This projection represents the hypothetical pollution penalty that would be associated with increased income if wealthy cities were to pollute at the same rate-per-income as poor cities. If the wealthiest cities in the model (Springfield, MA; Pittsburgh, PA; Minneapolis, MN) polluted at this projected rate, their NO_2 concentrations would be ~10× higher than modeled and observed levels.

To explore further the differences between developed and developing countries, we create "dummy" variables to define two income groupings using the World Bank's economic classification (based on GDP per capita): a four-level grouping (low, middle-low, middle-high, and high income) and a two-level grouping (high income; not high income). Neither grouping was selected using a backward stepwise multiple linear regression ($p < 0.1$) suggesting that the income variable employed in the main results above provides a reasonable measure of income/development.

Daytime chemical removal of atmospheric NO_2 is governed by sunlight, yielding a latitudinal gradient in NO_2 concentrations. The absolute value of latitude is correlated with the logarithm of NO_2 (R^2 = 0.37) for the cities in our analysis. However, the latitudinal dependence is complicated by the fact that the majority of developed countries are located in Northern midlatitudes. To explore the effect of latitude on our results we first calculate the NO_2 latitudinal gradient over the open ocean (method: longitudinally averaged surface NO_2 using the 0.1° gridded estimates, over oceans). This gradient reaches its peak in the Northern midlatitudes, with NO_2 concentrations that are 0.3 ppb greater than in low latitudes. The standard deviation of NO_2 concentrations for the cities in our analysis is almost an order of magnitude greater (2.6 ppb), suggesting that the NO_2 differences seen among cities are much larger than those associated with latitude.

We consider three additional models using the logarithm of median, 90th percentile, and concentration-weighted mean NO_2 concentrations for the dependent variable. Model R^2 and p-values for independent variables are similar to results for the core model (see Table S2) indicating that our results are robust to the method chosen to spatially summarize urban NO_2 concentrations. Results using the 90th percentile of surface NO_2 concentration imply that population and urban contiguity have slightly greater importance (by 5−10%) for extreme NO_2 concentrations, i.e., pollution hot-spots, than for central-tendency NO_2 concentrations (see Table S2).

As another sensitivity analysis, we evaluated a model similar to Table 2 but with the dependent variable as the logarithm of arithmetic mean column (rather than surface) NO_2. Results are in Table S2. Model performance is good (R^2 = 0.70), and the unique effect of each independent variable (i.e., a plot analogous to Figure 2; not shown) is consistent with the core model. Thus, the modeled surface-to-column ratios do not appear to introduce differential bias into our core model.

Our findings indicate that cities with highly contiguous built-up areas have, on average, lower NO_2 concentrations. All else being equal, urban areas with large amounts of development detached from main built-up areas will tend to have higher NO_2 concentrations. The urban form metrics employed here do not allow us to distinguish among types of isolated development (e.g., residential-only subdivisions, versus satellite cities, versus business/industrial development) or their differential effect on NO_2. It is possible, for example, that *self-sufficient* isolated satellite cities might reduce travel and/or NO_2 concentrations. More work is needed in this regard. Overall our findings suggest that policies encouraging contiguous rather than isolated development may be an effective part of urban design strategies seeking to minimize NO_2 air pollution.

■ ASSOCIATED CONTENT

Ⓢ Supporting Information. Additional information on methods and model results (Figure S1 and Tables S1−S2). This material is available free of charge via the Internet at http://pubs.acs.org.

■ AUTHOR INFORMATION

Corresponding Author
*Phone: (612) 625-2397; fax: (612) 626-7750; e-mail: julian@umn.edu.

■ ACKNOWLEDGMENT

This work was supported by NSF-Division of Chemical, Bioengineering, Environmental, and Transport Systems (CBET) (grant 0853467). We acknowledge the free use of tropospheric NO_2 column data from the OMI sensor from www.temis.nl. We also acknowledge the NASA Global Modeling and Assimilation Office and the NASA GES DISC for the dissemination of MERRA data. We thank Heather Sander for her work in GIS generating coordinates for the built-up area of cities. We thank three anonymous reviewers for their feedback and insights.

■ REFERENCES

(1) Mathers, C. D.; Stevens, G.; Mascarenhas, M. *Global Health Risks: Mortality and Burden of Disease Attributable to Selected Major Risks*; World Health Organization: Geneva, Switzerland, 2009.

(2) United Nations. *World Urbanization Prospects: The 2007 Revision*; United Nations: New York, NY, 2008.

(3) U.S. Environmental Protection Agency, Office of Air Quality Planning and Standards. *National Air Quality: Status and Trends through 2007*; U.S. Environmental Protection Agency: Research Triangle Park, NC, 2008.

(4) World Health Organization. *Environment and Health in Developing Countries*; World Health Organization: Geneva, Switzerland, 2010.

(5) Bento, A. M.; Cropper, M. L.; Mobarak, A. M.; Vinha, K. The effects of urban spatial structure on travel demand in the United States. *Rev. Econ. Stat.* **2005**, *87* (3), 466–478.

(6) Cervero, R.; Radisch, C. Travel choices in pedestrian versus automobile oriented neighborhoods. *Transp. Policy* **1996**, *3* (3), 127–141.

(7) Dierkers, G.; Silsbe, E.; Stott, S.; Winkelman, S.; Wubben, M. *CCAP Transportation Emissions Guidebook, Part One: Land Use, Transit and Travel Demand Management*; Center for Clean Air Policy: Washington, DC, 2005.

(8) Giuliano, G.; Narayan, D. Another look at travel patterns and urban form: The U.S. and Great Britain. *Urban Stud.* **2003**, *40* (11), 2295–2312.

(9) Handy, S.; Cao, X.; Mokhtarian, P. Correlation or causality between the built environment and travel behavior? Evidence from Northern California. *Transport. Res.* **2005**, *10* (6), 427–444.

(10) Stone, B.; Mednick, A. C.; Holloway, T.; Spak, S. N. Is compact growth good for air quality? *J. Am. Plann. Assoc.* **2007**, *73* (4), 404–418.

(11) Boarnet, M. G.; Crane, R. *Travel by Design: The Influence of Urban Form on Travel*; Oxford University Press: New York, NY, 2001.

(12) Marshall, J. D. Energy-efficient urban form. *Environ. Sci. Technol.* **2008**, *42* (9), 3133–3137.

(13) Newman, P. W.; Kenworthy, J. R. Gasoline consumption and cities. *J. Am. Plann. Assoc.* **1989**, *55* (1), 24–37.

(14) Stone, B. Urban sprawl and air quality in large U.S. cities. *J. Environ. Manage.* **2008**, *86* (4), 688–698.

(15) Marshall, J. D.; McKone, T. E.; Deakin, E.; Nazaroff, W. W. Inhalation of motor vehicle emissions: Effects of urban population and land area. *Atmos. Environ.* **2005**, *39* (2), 283–295.

(16) Schweitzer, L.; Zhou, J. Neighborhood air quality, respiratory health, and vulnerable populations in compact and sprawled regions. *J. Am. Plann. Assoc.* **2010**, *76* (3), 363–371.

(17) Grossman, G. M.; Krueger, A. B. *Environmental Impacts of a North American Free Trade Agreement*; National Bureau of Economic Research: Cambridge, 1991.

(18) Shafik, N.; Bandyopadhyay, S. *Economic Growth and Environmental Quality: Time Series and Cross-Country Evidence*; The World Bank: Washington, DC, 1992.

(19) Panayotou, T. *Empirical Tests and Policy Analysis of Environmental Degradation at Different Stages of Economic Development*; World Employment Program, International Labour Office: Geneva, Switzerland, 1993.

(20) Arrow, K.; Bolin, B.; Costanza, R.; Dasgupta, P.; Folke, C.; Holling, C. S.; Jansson, B. O.; Levin, S.; Mäler, K. G.; Perrings, C.; Pimentel, D. Economic growth, carrying capacity, and the environment. *Ecol. Appl.* **1996**, *6* (1), 13–15.
(21) Leifman, M.; Heil, M. Guest editors' note. *J. Environ. Dev.* **2005**, *14* (1), 17–26.
(22) Marcotullio, P. J.; Williams, E.; Marshall, J. D. Faster, sooner, and more simultaneously: How recent road and air transportation CO_2 emission trends in developing countries differ from historic trends in the United States. *J. Environ. Dev.* **2005**, *14* (1), 125–148.
(23) Levelt, P. F.; van den Oord, G. H. J.; Dobber, M. R.; Mälkki, A.; Visser, H.; de Vries, J.; Stammes, P.; Lundell, J. O. V.; Saari, H. The Ozone Monitoring Instrument. *IEEE Trans. Geosci. Remote Sens.* **2006**, *44* (5), 1093–1101.
(24) Bandeira, J. M.; Coelho, M. C.; Elisa Sá, M.; Tavares, R.; Borrego, C. Impact of land use on urban mobility patterns, emissions and air quality in a Portuguese medium-sized city. *Sci. Total Environ.* **2011**, *409* (6), 1154–1163.
(25) Borrego, C.; Martins, H.; Tchepel, O.; Salmim, L.; Monteiro, A.; Miranda, A. I. How urban structure can affect city sustainability from an air quality perspective. *Environ. Modell. Software* **2006**, *21* (4), 461–467.
(26) De Ridder, K.; Lefebre, F.; Adriaensen, S.; Arnold, U.; Beckroege, W.; Bronner, C.; Damsgaard, O.; Dostal, I.; Dufek, J.; Hirsch, J.; IntPanis, L.; Kotek, Z.; Ramadier, T.; Thierry, A.; Vermoote, S.; Wania, A.; Weber, C. Simulating the impact of urban sprawl on air quality and population exposure in the German Ruhr area. Part II: Development and evaluation of an urban growth scenario. *Atmos. Environ.* **2008**, *42* (30), 7070–7077.
(27) Kahyaoğlu-Koračin, J.; Basset, S. D.; Mouat, D. A.; Gertler, A. W. Application of a scenario-based modeling system to evaluate the air quality impacts of future growth. *Atmos. Environ.* **2009**, *43* (5), 1021–1028.
(28) Song, J.; Webb, A.; Parmenter, B.; Allen, D. T.; McDonald-Buller, E. The impacts of urbanization on emissions and air quality: Comparison of four visions of Austin, Texas. *Environ. Sci. Technol.* **2008**, *42* (19), 7294–7300.
(29) Ewing, R.; Pendall, R.; Chen, D. Measuring sprawl and its transportation impacts. *Transp. Res. Rec.* **2007**, *1831* (2003), 175–183.
(30) Brauer, M.; Lencar, C.; Tamburic, L.; Koehoorn, M.; Demers, P.; Karr, C. A cohort study of traffic-related air pollution impacts on birth outcomes. *Environ. Health Perspect.* **2008**, *116* (5), 680–686.
(31) Castellsague, J.; Sunyer, J.; Saez, M.; Anto, J. M. Short-term association between air pollution and emergency room visits for asthma in Barcelona. *Thorax* **1995**, *50* (10), 1051–1056.
(32) Gauderman, W. J.; Avol, E.; Lurmann, F.; Kuenzli, N.; Gilliland, F.; Peters, J.; McConnell, R. Childhood asthma and exposure to traffic and nitrogen dioxide. *Epidemiology* **2005**, *16* (6), 737–743.
(33) Kim, J. J.; Smorodinsky, S.; Lipsett, M.; Singer, B. C.; Hodgson, A. T.; Ostro, B. Traffic-related air pollution near busy roads: The East Bay Children's Respiratory Health Study. *Am. J. Respir. Crit. Care Med.* **2004**, *170* (5), 520–526.
(34) Filleul, L.; Rondeau, V.; Vandentorren, S.; Le Moual, N.; Cantagrel, A.; Annesi-Maesano, I.; Charpin, D.; Declercq, C.; Neukirch, F.; Paris, C.; Vervloet, D.; Brochard, P.; Tessier, J. F.; Kauffmann, F.; Baldi, I. Twenty five year mortality and air pollution: Results from the French PAARC survey. *Occup. Environ. Med.* **2005**, *62* (7), 453–460.
(35) Beelen, R.; Hoek, G.; van den Brandt, P. A.; Goldbohm, R. A.; Fischer, P.; Schouten, L. J.; Jerrett, M.; Hughes, E.; Armstrong, B.; Brunekreef, B. Long-term effects of traffic-related air pollution on mortality in a Dutch cohort (NLCS-AIR study). *Environ. Health Perspect.* **2008**, *116* (2), 196–202.
(36) Krämer, U.; Herder, C.; Sugiri, D.; Strassburger, K.; Schikowski, T.; Ranft, U.; Rathmann, W. Traffic-related air pollution and incident type 2 diabetes: Results from the SALIA Cohort Study. *Environ. Health Perspect.* **2010**, *118* (9), 1273–1279.
(37) van Donkelaar, A.; Martin, R. V.; Brauer, M.; Kahn, R.; Levy, R.; Verduzco, C.; Villeneuve, P. J. Global estimates of ambient fine particulate matter concentrations from satellite-based aerosol optical depth: Development and application. *Environ. Health Perspect.* **2010**, *118* (6), 847–855.
(38) Martin, R. V. Satellite remote sensing of surface air quality. *Atmos. Environ.* **2008**, *42* (34), 7823–7843.
(39) Richter, A.; Burrows, J. P.; Nuss, H.; Granier, C.; Niemeier, V. Increase in tropospheric nitrogen dioxide over China observed from space. *Nature* **2005**, *437* (7055), 129–132.
(40) Lamsal, L. N.; Martin, R. V.; van Donkelaar, A.; Steinbacher, M.; Celarier, E. A.; Bucsela, E.; Dunlea, E. J.; Pinto, J. P. Ground-level nitrogen dioxide concentrations inferred from the satellite-borne Ozone Monitoring Instrument. *J. Geophys. Res.* **2008**, *113* (D16308); 10.1029/2007JD009235.
(41) Marshall, J. Megacity, mega mess. *Nature* **2005**, *437* (7057), 312–314.
(42) Andrews, S. Q. Inconsistencies in air quality metrics: 'Blue Sky' days and PM_{10} concentrations in Bejing. *Environ. Res. Lett.* **2008**, *3* (034009); 10.1088/1748−9326/3/3/034009.
(43) Hudman, R. C.; Jacob, D. J.; Turquety, S.; Leibensperger, E. M.; Murray, L. T.; Wu, S.; Gilliland, A. B.; Avery, M.; Bertram, T. H.; Brune, W.; Cohen, R. C.; Dibb, J. E.; Flocke, F. M.; Fried, A.; Holloway, J.; Neuman, J. A.; Orville, R.; Perring, A.; Ren, X.; Sachse, G. W.; Singh, H. B.; Swanson, A.; Wooldridge, P. J. Surface and lightning sources of nitrogen oxides over the United States: Magnitudes, chemical evolution, and outflow. *J. Geophys. Res.* **2007**, *112* (D12S05); 10.1029/2006JD007912.
(44) Angel, S.; Sheppard, S. C.; Civco, D. L. *The Dynamics of Global Urban Expansion*; The World Bank: Washington, DC, 2005.
(45) Potere, D.; Schneider, A.; Angel, S.; Civco, D. L. Mapping urban areas on a global scale: Which of the eight maps now available is more accurate? *Int. J. Remote Sens.* **2009**, *30* (24), 6531–6558.
(46) Barbier, E. B. Introduction to the environmental Kuznets curve special issue. *Environ. Dev. Econ.* **1997**, *2* (4), 369–381.
(47) Cole, M. A.; Rayner, A. J.; Bates, J. M. The environmental Kuznets curve: An empirical analysis. *Environ. Dev. Econ.* **1997**, *2* (4), 401–416.
(48) Selden, T. M.; Song, D. Environmental quality and development: Is there a Kuznets curve for air pollution emissions? *J. Environ. Econ. Manage.* **1994**, *27* (2), 147–162.
(49) Grossman, G. M.; Krueger, A. B. Economic growth and the environment. *Q. J. Econ.* **1995**, *110* (2), 353–377.
(50) Panayotou, T. Demystifying the environmental Kuznets curve: Turning a black box into a policy tool. *Environ. Dev. Econ.* **1997**, *2* (4), 468–484.
(51) Shafik, N. Economic development and environmental quality: An econometric analysis. *Oxford Econ. Pap.* **1994**, *46* (Special Issue on Environmental Economics), 757−773.

Supporting Information

Effects of income and urban form on urban NO_2: Global evidence from satellites

Matthew J. Bechle[1], Dylan B. Millet[1,2], Julian D. Marshall[1]

[1]*Department of Civil Engineering, University of Minnesota, Minneapolis, MN 55455*

[2]*Department of Soil, Water, and Climate, University of Minnesota, Minneapolis, MN 55455*

Methods

Satellite data. The Ozone Monitoring Instrument (OMI) onboard the Earth Observing System (EOS) Aura satellite (1) provides daily global measurements of total tropospheric NO_2 abundance. Aura's sun-synchronous orbit passes over the equator at ~13:45 local time (1). The OMI instrument has a 114° viewing angle (~2600 km wide swath) with 60 cross track measurements along the swath; resolution at nadir is up to 13×24 km^2. We employed the DOMINO standard product (Version 1.0.3, Collection 3) from the TEMIS project website (http://temis.nl). Errors in the tropospheric NO_2 product are mainly associated with uncertainties in surface albedo, aerosols, cloud parameters, and NO_2 profile (2). Additional uncertainty results from the separation of stratospheric and tropospheric NO_2, resulting in an overall error of up to 5% for clear scenes and up to 30-60% for scenes in the presence of clouds and pollution (2). To minimize errors associated with cloud cover, we used only cloud-free scenes (cloud radiance fraction < 0.3). To reduce spatial averaging near the swath edge, scenes are limited by pixel area (maximum: 50×24 km^2) and solar zenith angle (maximum: 85°). We eliminated measurements with a root mean square error of fit greater than 0.0003 and according to data-quality flags provided with the retrieval.

Previous work by Lamsal et al. (3) developed a method for inferring surface NO_2 concentrations from OMI column measurements, on the basis of local NO_2 vertical profiles simulated using a three-dimensional atmospheric model. We apply this approach here, using the GEOS-Chem chemical transport model (CTM) to simulate global NO_2 abundance and surface-to-column ratios for a 3-hour window (12:00-15:00 local time) corresponding to satellite overpass time for each city in the analysis. GEOS-Chem (version 8, http://www.geos-chem.org) uses GEOS-5 assimilated meteorological data from the NASA Goddard Earth Observing System, which have 6-h temporal resolution (3-h for surface variables and mixing depths), 0.5°×0.667° horizontal resolution, and 72 vertical layers. For computational expediency we degrade the horizontal resolution here to 2°×2.5° and the vertical resolution to 47 vertical layers. The model includes detailed ozone-NO_x-VOC chemistry coupled to aerosols, with 120 species simulated explicitly. Further details regarding the model simulation for NO_2 and related species, including evaluation against aircraft and surface data, are provided elsewhere (4). The satellite-based NO_2 estimates employed here reflect ambient, not exposure, concentrations.

Lamsal et al. (3) demonstrated that the approach employed here to derive surface NO_2 concentrations from the satellite data gives values that are well-correlated with in-situ observations, and with <30% bias. Our own (unpublished) comparisons indicate that urban-scale NO_2 variability across the South Coast Air Basin in California is well-resolved using surface concentrations estimated in this way from the OMI data and GEOS-Chem (r = 0.74 versus in-situ monitors). Both of these findings provide support for our use of OMI in combination with GEOS-Chem to examine differences in average NO_2 among cities.

Three years (2005-2007) of daily estimated ground-level NO_2 concentration was binned to a 0.1°×0.1° global grid (~11×11 km^2 at the equator), resulting in a spatial resolution smaller than that of the nadir scenes. All grid cells falling within an OMI pixel were assigned the measured tropospheric abundance for that pixel. In the case of overlapping OMI scenes for one day, a weighted average was taken; the weighting factor (w), adopted from Wenig et al. (5), takes into account the fractional cloud cover (C) and pixel area (A):

$$w = \frac{1}{A(1+3C)^2} \tag{1}$$

Meteorological data. Meteorological data were obtained from the Modern Era Retrospective-analysis for Research Application (MERRA) provided by NASA's

Global Modeling and Assimilation Office (GMAO) (publicly available at http://disc.sci.gsfc.nasa.gov/daac-bin/DataHoldings.pl). Horizontal components of wind speed (u) and mixing height (H) were obtained at 0.5°×0.667° for the study period (2005-2007). The average wind speed over the mixed layer was calculated using a power-law wind velocity profile. Hourly-average data were linearly interpolated to 0.1 hour increments for the overpass time (12:00-15:00 local time), with data selected for each built-up area pixel (0.1×0.1 km^2) using the nearest grid cell. The harmonic temporal mean of the dilution rate (uH) for the overpass time (12:00-15:00 local time) was determined for each built-up area pixel, and the spatial mean of that quantity over all built-up pixels used as a meteorology metric for each city.

Urban-level NO_2 and regression analysis. We interpolated ground-level NO_2 estimates (0.1°×0.1°) derived from the satellite data to a 0.1×0.1 km^2 grid of built-up land for each urban area via inverse distance-weighting of the three nearest grid cells. Three-year annual average mixing ratios were then computed for each metropolitan area using four spatial summaries (arithmetic mean, median, 90th percentile, and concentration-weighted mean); in each case, NO_2 concentrations are log-normally distributed among cities (basis: Shapiro-Wilks test; Shapiro-Francia test). Linear regression hypothesis-testing and confidence interval derivation both assume normality and homoscedacity in the dependent variable (6), assumptions which are violated with the non-transformed urban NO_2 concentrations but satisfied with the log-transformed data. We accordingly used the base-10 logarithm of NO_2 concentration as the dependent variable in the models. (A model developed using mean NO_2 concentrations rather than log-transformed values [not shown] exhibits poorer performance than other models [R^2=0.36, adj-R^2=0.31] and violates homoscedacity requirements.) The primary linear regression model given in the main text, which is for the arithmetic mean concentration, is shown in Fig. S1. That model plus four other models (dependent variables: median concentration, 90th percentile concentration, concentration-weighted mean, arithmetic mean column abundance) are in Table S2.

Figures

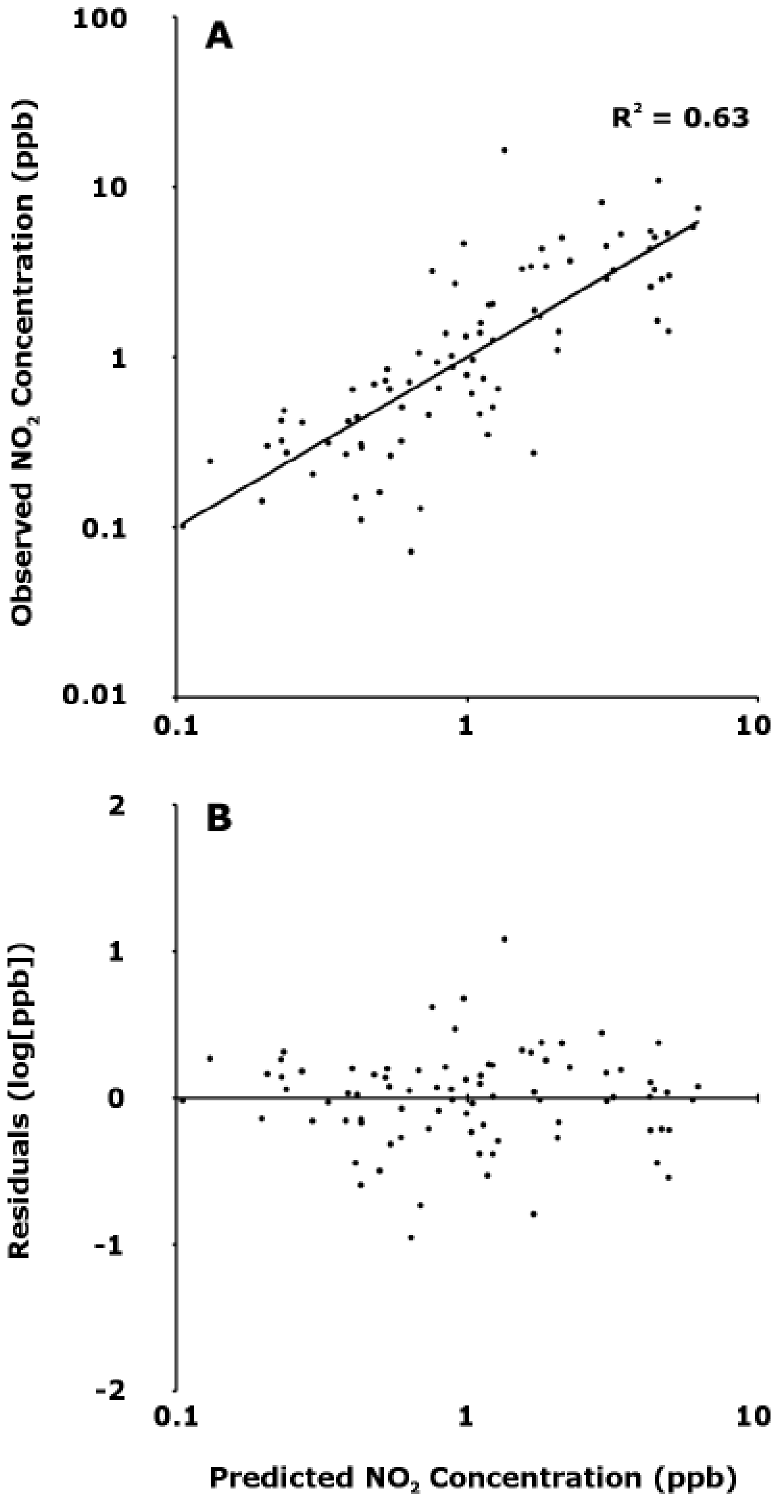

Figure S1. Core linear regression model for predicting logarithm of arithmetic mean NO_2 concentration. (A) Predicted vs. observed concentrations. (B) Model residuals.

Tables

Table S1: Summary Statistics among the 83 Cities

	Mean	**SD**[a]	**GM**[b]	**GSD**[c]	**Interquartile range**
Arithmetic mean NO_2 (ppb)	2.0	2.6	1.0	3.4	0.41 – 3.0
Median NO_2 (ppb)	2.1	2.8	1.0	3.5	0.42 – 3.1
90th percentile NO_2 (ppb)	2.4	3.2	1.1	3.5	0.43 – 3.5
Conc.-weighted NO_2 (ppb)	2.1	2.7	1.0	3.4	0.42 – 3.2
Arithmetic mean column NO_2 (10^{15} molec cm^{-2})	5.2	5.1	3.5	2.4	1.7 – 7.5
Population (million)	2.7	3.8	1.3	3.0	0.56 – 2.8
Income (US$)	$9,600	$10,000	$5,400	3.3	$2,300 - $18,000
Contiguity index	0.71	0.20	0.67	1.4	0.59 – 0.89
Compactness index	0.35	0.10	0.33	1.4	0.27 – 0.43
Harmonic mean dilution rate (m^2 s^{-1})	2,600	2,600	1,500	3.1	520 – 4,300

[a] Standard deviation. [b] Geometric mean. [c] Geometric standard deviation, unitless.

Table S2: Linear Regression Model Results

Dependent variable	Independent variable	Coeff.	Std. error	$P<\lvert t \rvert$	Δ (1-SD↑)[a]	Δ(1-SD↓)[a]
	constant	-2.4	0.47	<0.001	--	--
	Income (US$)	6.5e-05	1.7e-05	<0.001	} -22%	-22%
Log of arithmetic mean NO_2[b]	$(\text{Income})^2$	-1.1e-09	5.5e-10	0.05		
	Log(population)	0.41	0.074	<0.001	62%	-38%
$R^2 = 0.63$	Contiguity	-0.58	0.19	0.004	-24%	31%
Adj. $R^2 = 0.60$	Compactness	0.19	0.37	0.62	4.6%	-4.4%
	Dilution rate ($m^2\ s^{-1}$)	-4.6e-05	1.5e-05	0.003	-24%	31%
	constant	-2.5	0.48	<0.001	--	--
	Income (US$)	6.5e-05	1.7e-05	<0.001	} -23%	-23%
Log of median NO_2	$(\text{Income})^2$	-1.1e-9	5.5e-10	0.05		
	Log(population)	0.42	0.075	<0.001	64%	-39%
$R^2 = 0.63$	Contiguity	-0.58	0.20	0.004	-24%	31%
Adj. $R^2 = 0.60$	Compactness	0.16	0..38	0.66	4.1%	-3.9%
	Dilution rate ($m^2\ s^{-1}$)	-4.6e-05	1.5e-05	0.003	-24%	31%
Log of 90th percentile NO_2	_constant_	-2.5	0.48	<0.001	--	--
	Income (US$)	6.4e-05	1.7e-05	<0.001	} -22%	-22%
$R^2 = 0.64$	$(\text{Income})^2$	-1.1e-09	5.5e-10	0.06		
Adj. $R^2 = 0.62$	Log(population)	0.43	0.074	<0.001	67%	-40%

	Contiguity	-0.63	0.19	0.002	-26%	-34%
	Compactness	0.12	0.37	0.75	3.0%	-2.9%
	Dilution rate (m^2 s^{-1})	-4.7e-05	1.5e-05	0.002	-24%	32%
Log of concentration-weighted NO_2	_constant_	-2.5	0.47	<0.001	--	--
R^2 = 0.63	Income (US$)	6.5e-05	1.7e-05	<0.001	-22%	-22%
Adj. R^2 = 0.61	$(\text{Income})^2$	-1.1e-09	5.5e-10	0.05		
	Log(population)	0.41	0.074	<0.001	64%	-39%
	Contiguity	-0.58	0.19	0.003	-24%	31%
	Compactness	0.16	0.37	0.37	3.9%	-3.9%
	Dilution rate (m^2 s^{-1})	-4.7e-05	1.5e-05	0.003	-24%	32%
Log of arithmetic mean column NO_2	_constant_	-1.7	0.31	<0.001	--	--
R^2 = 0.70	Income (US$)	4.5e-05	1.1e-05	<0.001	-17%	-17%
Adj. R^2 = 0.68	$(\text{Income})^2$	-7.9e-10	3.6e-10	0.03		
	Log(population)	0.38	0.05	<0.001	58%	-37%
	Contiguity	-0.41	0.13	0.002	-17%	21%
	Compactness	0.04	0.24	0.87	1.0%	-1.0%
	Dilution rate (m^2 s^{-1})	-3.3e-05	9.8e-06	0.001	-18%	21%

[a] Percent change for a one standard deviation increase/decrease from mean value while all other independent variables are held at mean value. For income, percent change for a one standard deviation increase/decrease from peak NO_2 value while all other independent variables are held at mean value.

[b] Core model.

References

S1. Levelt, P. F.; van den Oord, G. H. J.; Dobber, M. R.; Mälkki, A.; Visser, H.; de Vries, J.; Stammes, P.; Lundell, J. O. V.; Saari, H. The Ozone Monitoring Instrument. *IEEE Trans. Geosci. Remote Sens.* **2006**, *44* (5), 1093-1101.

S2. Boersma, K. F.; Bucsela, E. J.; Brinksma, E. J.; Gleason, J. F. NO_2 in *OMI Algorithm Theoretical Basis Document: OMI Trace Gas Algorithms*; Chance, K. Ed.; Smithsonian Astrophysical Observatory: Cambridge, MA, 2002.

S3. Lamsal, L. N.; Martin, R. V.; van Donkelaar, A.; Steinbacher, M.; Celarier, E. A.; Bucsela, E.; Dunlea, E .J.; Pinto, J. P. Ground-level nitrogen dioxide concentrations inferred from the satellite-borne Ozone Monitoring Instrument. *J. Geophys. Res.* **2008**, *113* **(**D16308); 10.1029/2007JD009235.

S4. Hudman, R. C.; Jacob, D. J.; Turquety, S.; Leibensperger, E. M.; Murray, L. T.; Wu, S.; Gilliland, A. B.; Avery, M.; Bertram, T. H.; Brune, W.; Cohen, R. C.; Dibb, J. E.; Flocke, F. M.; Fried, A.; Holloway, J.; Neuman, J. A.; Orville, R.; Perring, A.; Ren, X.; Sachse, G. W.; Singh, H. B.; Swanson, A.; Wooldridge, P. J. Surface and lightning sources of nitrogen oxides over the United States: Magnitudes, chemical evolution, and outflow. *J. Geophys. Res.* **2007**, *112* (D12S05); 10.1029/2006JD007912.

S5. Wenig, M.O.; Cede, A. M.; Buscela, E. J.; Celarier, E. A.; Boersma, K. F.; Veefkind, J. P.; Brinksma, E. J.; Gleason, J. F.; Herman, J. R. Validation of OMI tropospheric NO_2 column densities using direct-Sun mode Brewer measurements at NASA Goddard Space Flight Center. *J. Geophys. Res. 113* (D16S45); 10.1029/2007JD008988.

S6. Zar, J. H. *Biostatistical Analysis, 4th Ed*; Prentice Hall: Upper Saddle River, NJ, 1998.